Journal of Applied Pharmaceutical Science Vol. 5 (Suppl 2), pp. 037-044, 2015
Available online at http://www.japsonline.com
DOI: 10.7324/JAPS.2015.58.S6
ISSN 2231-3354

Interaction of Ketoconazole with Bovine Serum Albumin: Electrochemical, Spectroscopic and Molecular Modeling Studies

Babu Gowda*, Mallappa M., Jayant I. Gowda, Raghavendran Rengasamy

Department of Chemistry, Maharani's Science College for Women, Bangalore-560 001, India.
Department of studies in Chemistry, Karnatak University, Dharwad, India.
DBT-Bioinformatics Infrastructure Facility, Maharani's Science College for Women, Bangalore-560 001, India.

ARTICLE INFO

Article history:
Received on: 24/03/2015
Revised on: 22/04/2015
Accepted on: 14/05/2015
Available online: 04/09/2015

Key words:
Ketoconazole, bovine serum albumin, voltammetry, spectroscopy and molecular modeling

ABSTRACT

The interaction of ketoconazole (KTZ) with bovine serum albumin (BSA) has been investigated by cyclic voltammetry, differential pulse voltammetry, UV-Vis absorption and fluorescence spectroscopy, viscosity measurements as well as molecular modeling methods. The measurements were performed in 0.1 mol L^{-1} phosphat buffer solution at pH = 7.4. Shifts in the peak potentials in cyclic Voltammetry, spectral changes in UV absorption and fluorescence titration, an increase in viscosity of BSA and the molecular modeling methods strongly support the electrostatic interaction between KTZ and BSA. The thermodynamic parameters ΔH, ΔG and ΔS at different temperatures were calculated, showing that the electrostatic interactions and hydrophobic interaction are the main forces for the binding of KTZ to BSA. The binding constant (K_b) determined by UV absorption and fluorescence measurements are very close to the value determined by cyclic Voltammetry assuming that the binding equilibrium is static. Moreover, from molecular modeling method, a docked structure with minimum energy was obtained in which KTZ was located in minor grooves of BSA.

INTRODUCTION

Ketoconazole (Figure 1) is one of the most famous antifungal medications and a potent inhibitor against the enzyme cytochrome P450 (CYP3A4); several statins, including simvastatin and lovastatin, interact with this hepatic microsomal enzyme, which is responsible in significant part for statin clearance (Feely, 2001). It is often used to treat fungal infections that can spread to different parts of the body through the bloodstream such as yeast infections of the mouth, skin, urinary tract, and blood, and certain fungal infections that begin on the skin or in the lungs and can spread through the body. KTZ works by slowing the growth of fungi which may cause infection. It is used to treat a variety of fungal infections such as candida infections of the skin or mouth (thrush), blastomycosis, histoplasmosis, coccidiomycosis, and others. Protein is an important component of cell and the executor of life activities. It is a frontier topic to study the function of protein in life science. Studying the thermodynamics characteristics and mechanism of the interaction of a small organic molecule such as medicament with biological macromolecules is an important component of life sciences. Serum albumins are the most abundant proteins in plasma (Carter *et al.*, 1994). As the major soluble protein constituents of the circulatory system, they have many physiological functions. They contribute to colloid osmotic blood pressure and are primarily responsible for the maintenance of blood pH (He *et al.*, 1994, Zolese *et al.*,2000, Chadborn *et al.*, 1994) they can play a dominant role in drug metabolism, efficacy and disposition (Eson *et al.*,1996). Many drugs and other bioactive small molecules bind reversibly to albumin (Hu *et al.*,2005, Hu *et al.*,2004, Guharay *et al.*, 2001), which implicates a serum albumin role as carriers. Consequently, it is important to study the interactions of drugs with this protein.

These studies may provide information about the structural features that determine the therapeutic effectiveness of drugs, and have become an important research field in the life sciences, chemistry and clinical medicine. In this work, BSA was selected as our protein model because of its medical importance, low cost, ready availability, unusual ligand binding properties, and the results of all the studies are consistent with the fact that bovine and human serum albumins are homologous proteins (Chadborn *et al.*, 1994; Brockhinke *et al.*, 2003).

* *Corresponding Author*
Babu Gowda, Department of Chemistry, Maharani's Science College for Women, Bangalore-560 001, India
Email: babgowda@gmail.com

In recent years, there has been a growing interest in the CV investigations of the interactions between drugs and proteins. Observing the pre- and post-electrochemical signals of proteins provides good evidence for determining the interaction mechanism.

An electrochemical approach can provide new insight into rational drug design and would lead to increased understanding of the interaction mechanism between drugs and proteins. Spectroscopy (fluorescence and UV-vis. Spectroscopy) is also a powerful tool for the study of the reaction of chemical and biological systems since it allows non-intrusive measurements of substances at a low concentration under physiological conditions (Lakowicz JR *et al.,* 1999).

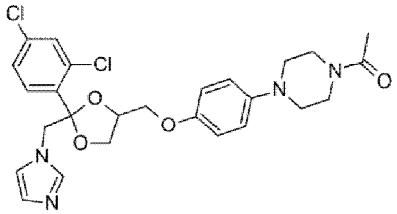

Fig.1: Chemical structure of Ketoconazole.

Quenching measurement of albumin fluorescence is an important method to study the interactions of drugs with protein (Klajnert *et al.,* 2002, Sulkowska *et al.,* 2003). The effectiveness of drugs depends on their binding ability with albumins, so it is significant to study the interactions of drugs with proteins. These studies can reveal the accessibility of quenchers to albumin fluorophore groups, help to understand albumin binding mechanisms to drugs, and provide clues to the nature of the binding phenomenon.

Moreover, molecular docking techniques play an important role in drug design and were applied to describe the most probable mode of protein binding. When used prior to experimental screening, DOCK, AutoDock and molecular operating environment (MOE) can be considered powerful computational filters and enable a reduction in the cost and labour required for the development of potent medicinal drugs. Docking techniques will undoubtedly continue to play an important role in drug discovery.

In the present work, we demonstrated the interactions between KTZ and BSA by electrochemical, spectroscopic, viscometric and molecular modeling methods. The aim of our work was to determine the affinity of KTZ for BSA, and to investigate the thermodynamics of their interaction.

MATERIALS and METHODS

Apparatus and Reagents

All of the fluorescence measurements were carried out on a F-2700 recording spectrofluorometer (Hitachi, Japan) equipped with a 150 W Xenon lamp source and 1.0 cm quartz cells. The excitation and emission bandwidths were both 5 nm. An Ellico UV-visible spectrophotometer equipped with a 1.0 cm cuvette was used to scan the UV spectrum. All of the pH measurements were made with an Elico LI120 digital pH meter (Elico Ltd., India). The viscosity measurements were made with viscometer which was immersed in a thermostat water-bath at room temperature.

Bovine serum albumin (BSA) was purchased from Sigma Chemical Company, St. Louis, USA and used without purification. A 99.99% pure ketokonazole (KTZ) was obtained from Cipla Ltd., India. The solutions of KTZ and BSA were prepared in 0.1 M phosphate buffer of pH 7.4 with respect to their molecular weight. All other chemicals were of analytical reagent grade and Millipore water was used throughout the work.

Molecular docking

The molecular docking studies were performed by using Auto dock Vina, developed at the Scripps research institute (http://vina.scripps.edu) (Morris *et al.,* 1998). The input files for AutoDock Vina were prepared with AutoDock Tools (ADT), which is a Graphical User Interface for AutoDock and AutoDock Vina. The Grid box has been set according to the binding site on protein and saved as pdbqt format, which was required by AutoDock Vina.

The structure of KTZ was sketched by CHEMSKECTH (http://www.acdlabs.com) and converts into pdb format from mol format by OPENBABEL (http://www.vcclab.org/lab/babel/) (Noel *et al.,* 2011). The crystal structure of BSA (3V03) is obtained from the Protein Data Bank (http://www.rcsb.org./pdb) and the ligand binding site location was analyzed by Q-Site Finder (Alasdair *et al.,* 2005). The co crystallized ligand was removed. Using ADT the water molecules were removed from the protein and polar hydrogen were added followed by adding Kollman charges. The rotatable bonds were selected within the ligand using Choose Torsions option in ADT and saved in pdbqt format. The Lamarckian Genetic Algorithm (LGA), which is a novel and robust automated docking method available in AutoDock (Trott O *et al.,* 2010), was employed.

RESULTS AND DISCUSSIONS

Voltammetric behaviour of KTZ at a GCE

The electrochemical behaviour of KTZ (1.0×10^{-3} M) at a GCE was investigated by CV. KTZ showed one oxidation peak at 0.667 V with corresponding peak current -2.202 µA in PBS buffer of pH 7.4 with a scan rate of 50 mV s^{-1} (Figure 2a). No peak was observed in the reverse scan, suggesting that the oxidation of KTZ on the GCE was irreversible. Multi-sweep cyclic voltammogram of KTZ (data not shown) revealed a significant decrease in peak current, indicating fouling of the electrode surface due to adsorption of KTZ or its oxidation product.

For an irreversible process, the number of electron transfer (n) could be obtained by Eq. (1) (Bard A J *et al.,* 1980).

$$\Delta E_{pa} = E_{pa} - E_{pa/2} = (47.7/\alpha n)\ \text{mV (at 298 K)} \quad (1)$$

Where $E_{pa/2}$ is the half peak potential, α represents the electron transfer coefficient (generally, $0.3 < \alpha < 0.7$), α is assumed to be

0.5 for a totally irreversible process. In this study, a value of 47 mV for $|Epa-Epa_{/2}|$ is obtained from equation 1 and the value of n is 2.029 (≈ 2) is yielded referring to Eq. (1) (Stela *et al.*, 2011). Therefore, the electrochemical oxidation of KTZ undergoes $2e^-$ transfer process.

Based on the above results, it is proposed that during electrooxidation, KTZ involves two protons and two electrons oxidation to yield substituted ketone adduct, due to an oxidation mechanism (Scheme 1) similar to caffiene. This is also in agreement with an earlier report (Biris *et al.*, 2011).

For an irreversible oxidation reaction, the following equation was used to calculate standard rate constant (k_0) (Kalanur *et al.*, 201, Laviron *et al.*, 1974).

$$E_p = E^0 + (RT/\alpha nF)\,[ln\,(RTk_0/\alpha nF)] - ln\nu \qquad (2)$$

Where E_0 is the formal potential, R is the universal gas constant (8.314 J K^{-1} mol^{-1}), T (K) was the Kelvin temperature, α is the transfer coefficient, k_0 (s^{-1}) is the electrochemical rate constant and F was the Faraday constant (96,487 C mol^{-1}). The value of E^0 was obtained from the intercept of E_p *vs ln ν* plot by the extrapolation to the vertical axis at ν = 0. The k_0 value, 1.27 x 10^2 s^{-1} was evaluated from the plot of E_p *vs* ln ν.

Influence of scan rate on electrooxidation of KTZ

We examined the influence of the scan rate on the electrochemical behaviour of KTZ, to understand the nature of the electrode process. For this, we recorded cyclic voltammogram of 1.5 x 10^{-4} M KTZ at a GCE at different scan rates (Figure 2a). The oxidation peak current of KTZ was noted to increase with increasing scan rate, with a positive shift in the peak potential. The plot of values of log I_p versus log ν in the scan rate range of 25 - 300 mV s^{-1} yielded a straight line with a slope of 0.532. This value is close to the theoretical value of 0.5 expected for an ideal reaction condition for a diffusion-controlled electrode process (Bard *et al.*, 1980).

In addition, the graphs of I_{pa} versus ν and I_{pa} versus $\nu^{1/2}$ (Fig. 2b and 2c) have good linearity. In the range from 25 to 300 mVs^{-1}, the anodic peak currents were proportional to the scan rate. The correlation coefficient was found to be -0.9979 (n = 12) and -0.98221 (n = 12), which indicates the electrode reaction was diffusion controlled.

Voltammetric studies of KTZ–BSA interaction

CV and DPV of 1.5 x 10^{-4} M KTZ in absence and presence of BSA on GCE in PBS buffer of pH 7.4 are shown in Fig 3(a) and 3(b). The voltammogram without BSA shows stable anodic peak in the potential range of 0.2 - 1.0 V. The anodic peak was appeared at 0.667 V versus SCE corresponding peak current is -2.202 µA. By the addition of 10 - 180 µM of BSA the anodic peak potential was shifted to negative direction and also anodic peak current (I_{pa}) was decreased. The significant decrease in peak current is attributed to the formation of slowly diffusing KTZ-BSA supramolecular complex due to which the concentration of the free drug, which is responsible for the transfer of current is lowered. The calculated value of k_0 is found to be 1.27 x 10^2 s^{-1} in the absence of BSA and 1.38 x 10^2 s^{-1} in presence of BSA. In this way, appreciable difference in the value of k_0 in presence and absence of BSA was not observed indicating that the BSA did not alter the electrochemical kinetics of KTZ oxidation.

In general the positive shift in potential is caused by the intercalation of the drug into the double helical structure of BSA (Laviron E. 1979), while negative shift is observed for the electrostatic interaction of the cationic drug with the anionic phosphate of BSA backbone (Aslanoglu, 2006). So the obvious negative peak potential shift in the CV and DPV of KTZ by the addition of BSA is attributable to the electrostatic interaction of KTZ with BSA. The cathodic peak potential shift indicates the easier oxidation of KTZ in presence of BSA because its oxidized form is more strongly bound to BSA than its reduced form. According to the decrease in peak current of KTZ by the addition of different concentration of BSA, the binding constant was calculated according to the following equation (Li *et al.*, 2005):

$$\frac{1}{[BSA]} = \frac{K\,(1-A)}{1 - (I/I_o)} - K \qquad (3)$$

Where, K is the binding constant, I and I_0 are the peak currents with and without BSA and A is the proportionality constant.

A plot of 1/ [1- (I_0/I)] versus 1/ [BSA] was constructed (Fig. 4a) and from the ratio of the intercept to slope, the value of K is calculated to be 1.24 x 10^4 L mol^{-1} (R^2 = 0.9999).

The binding constant and binding site size was determined using the following equation (Shah *et al.*, 2008):

$$\frac{C_b}{C_f} = K\left\{\frac{[\text{Free base pairs}]}{S}\right\} \qquad (4)$$

Where, S is the binding site size in terms of base pairs. Measuring the concentration of BSA in terms of [KTZ], the concentration of the base pairs can be expressed as [BSA]/2. Therefore, Eq. (4) can be written as:

$$\frac{C_b}{C_f} = K\left\{\frac{[BSA]}{2S}\right\} \qquad (5)$$

Therefore, C_f and C_b represent the concentrations of the free and BSA-bound species respectively. The C_b/C_f ratio was determined by the equation given below (Aslanoglu *et al.*, 2004),

$$\frac{C_b}{C_f} = \frac{I_0 - I}{I} \qquad (6)$$

Where, I and I_0 represent the peak currents of the drug in the presence and absence of BSA respectively.

Putting the value of 1.24 x 10^4 L mol^{-1} as calculated according to Eq. (3), the binding site size of 0.89 ≈ 1.0 bp was obtained from the plot (Fig. 4b) of C_b/C_f versus [BSA]. The small value of 'S' indicates electrostatic interaction of KTZ with BSA.

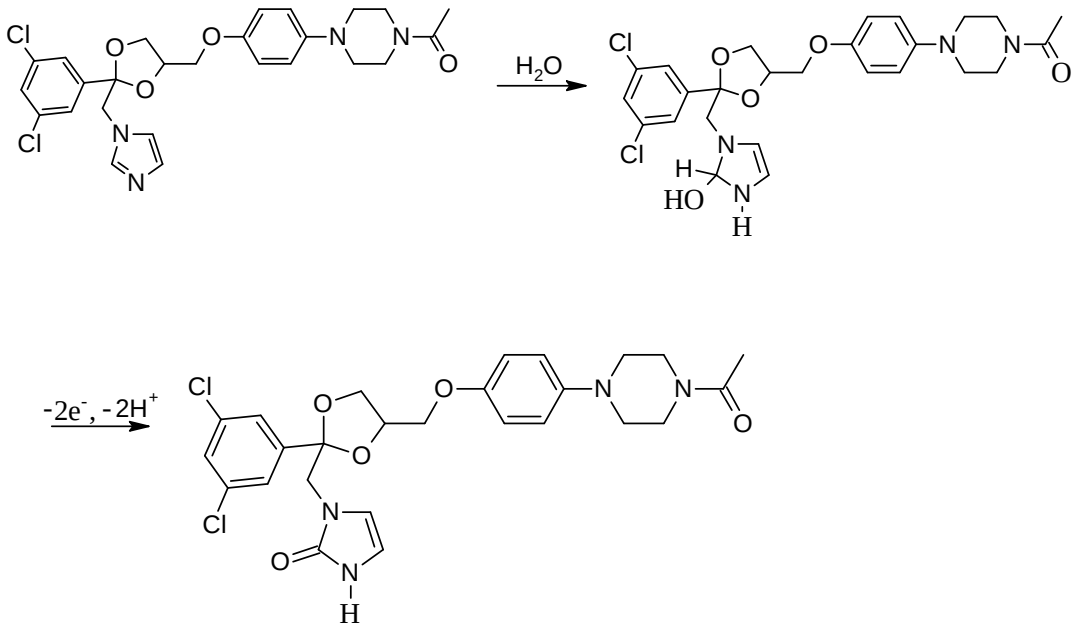

Scheme 1: Probable reaction mechanism for electrooxidation of KTZ.

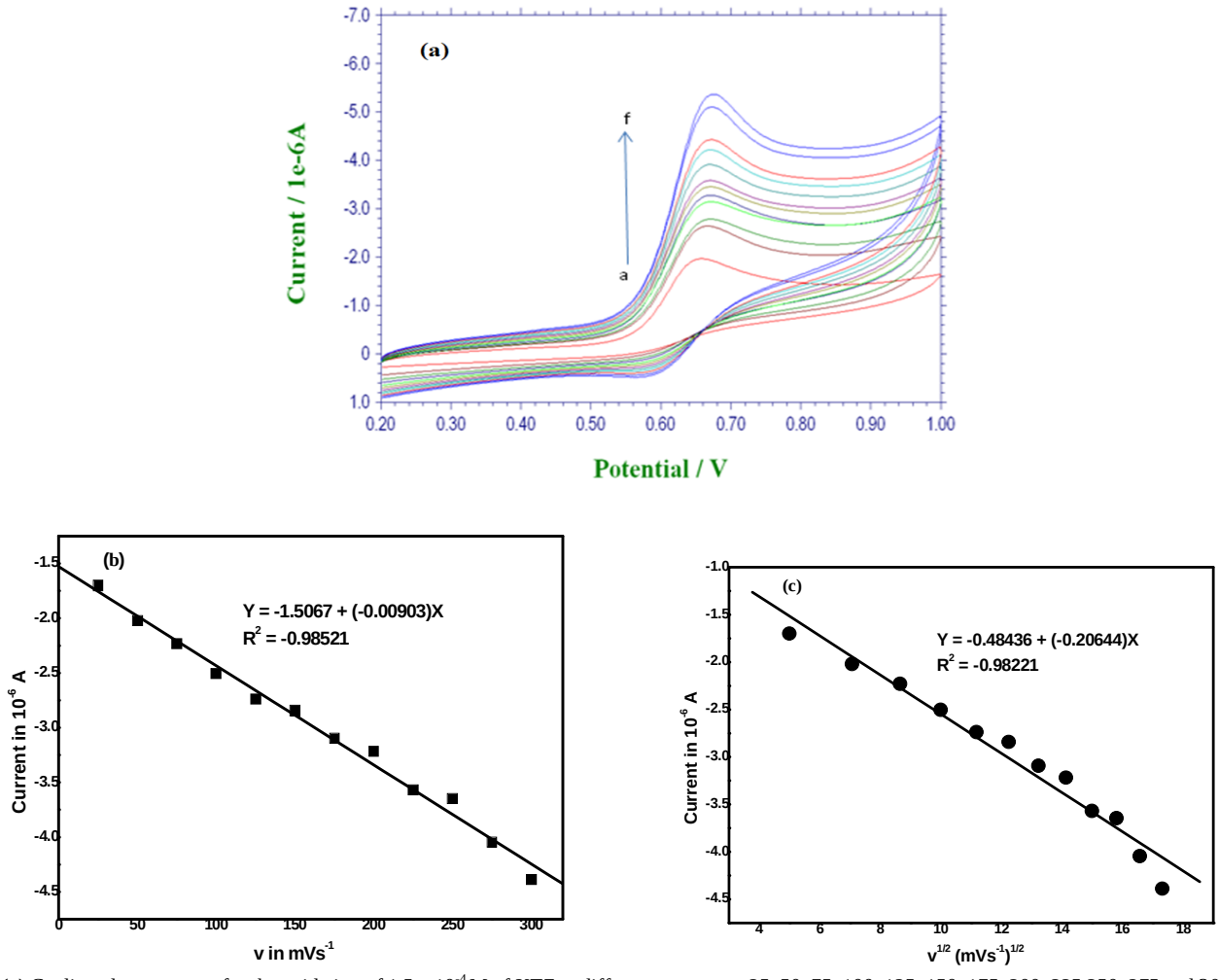

Fig. 2 (a) Cyclic voltammogram for the oxidation of 1.5 x 10^{-4} M of KTZ at different scan rates: 25, 50, 75, 100, 125, 150, 175, 200, 225 250, 275 and 300 mV s^{-1} (a–f). **(b)** Plot of I_{pa} versus v (**c**) Plot of I_{pa} versus $v^{1/2}$ of KTZ.

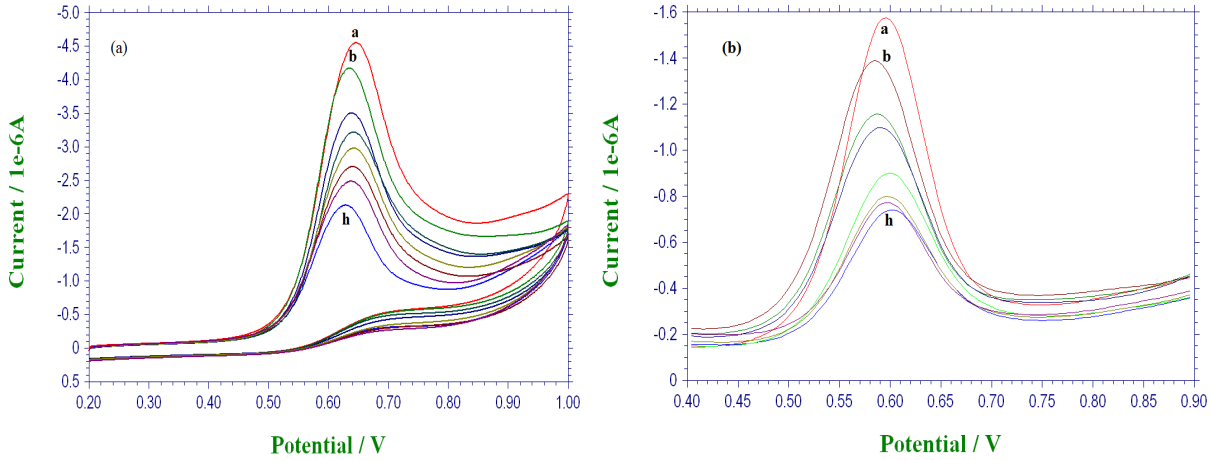

Fig. 3 (a) CV's and **(b)** DPV's of 1.5 x 10^{-4} M KTZ in presence of C_{BSA}= 0, 10, 50, 70, 100, 120, 150 and 180 µML^{-1} (b to h) in phosphate buffer of pH 7.4 at 50 mVs^{-1}

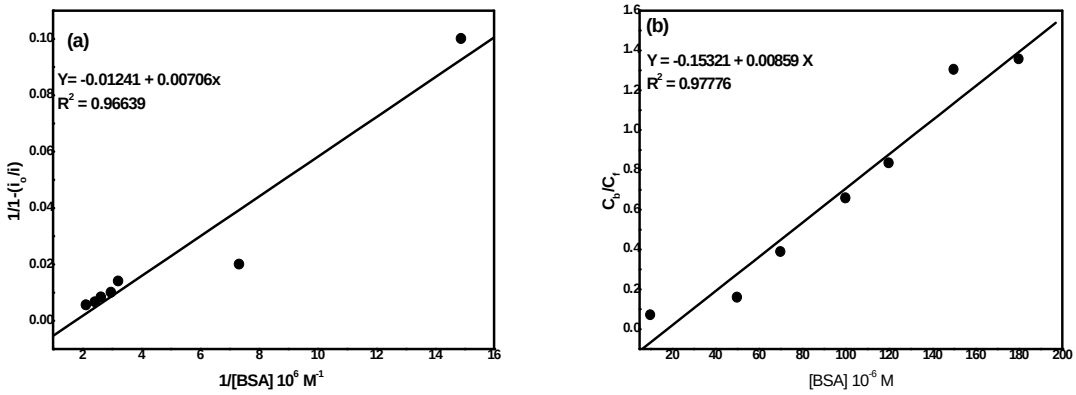

Fig. 4 (a): Plot of 1/ [1- (i_0/i)] versus 1/ [1- BSA]; **(b)** Plot of C_b /C_f versus [BSA]

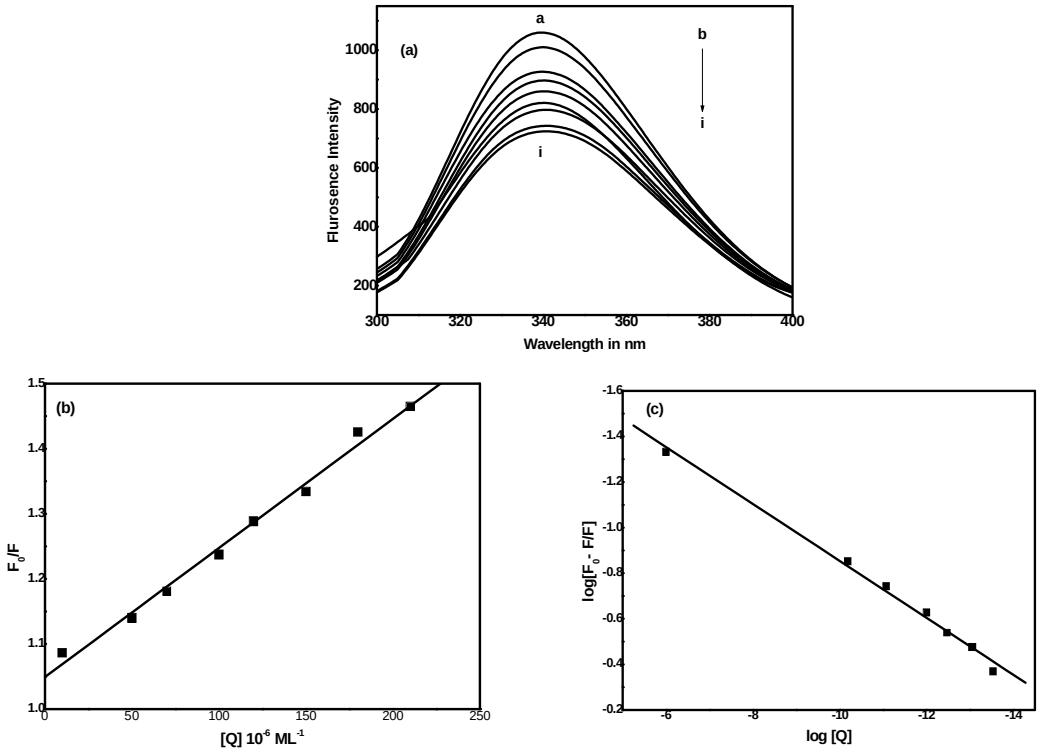

Fig. 5 (a) Florescence spectra of 1x10^{-5} M BSA in presence of C_{KTZ} = 0, 10, 50, 70, 100, 120, 150, 180 µML^{-1} (b to i) in PBS of pH 7.4, **(b)** Plot of F_0/F versus [BSA] and **(c)** Plot of log [(F_0-F)/F] versus log [BSA].

Table 1: Binding constants and thermodynamic parameters for the interaction of KTZ and BSA.

Temperature K	K_b x 10^4 M^{-1}	ΔH K J M^{-1}	ΔS J $M^{-1}K^{-1}$	ΔG K J M^{-1}	Linear regression	R^2
298	1.170		138.343	-24.263	Y=7.833+54.6182x	0.9982
303	1.966	-16.825	137.70	-24.898	Y= 6.678+ 51.0079x	0.9991
308	2.0		136.787	-25.442	Y=4.974+ 0.5859x	0.9985

Fluorescence spectral studies

Figure 5a shows the fluorescence spectra of KTZ and BSA. The fluorescence emission lines of the KTZ-BSA (1:1) mixture system can also be observed in Fig. 5a. The BSA showed a strong emission band centered at 338 nm when excited with a 285 nm wavelength. The concentration of BSA was stabilized at 1.0 x 10^{-5} mol L^{-1}. Regular decrease in fluorescence intensity of BSA is observed with increasing concentration of KTZ, which means that interaction has occurred and KTZ quenches the intrinsic fluorescence of BSA.

The quenching rate constant (k_q) was calculated according to Stern–Volmer equation: $F/F_0 = 1 + k_q\tau_0 [Q] = 1 + K_{SV} [Q]$, where F_0 and F are the fluorescence intensities in the absence and presence of BSA. K_{SV} is the Stern–Volmer quenching constant, [Q] is the concentration of BSA and τ_0 is the average fluorescence lifetime (~10^{-8} s). The plot of Stern–Volmer equation is shown in Fig. 5b, from which k_q was obtained to be 1.785 x 10^{12} L mol^{-1} s^{-1} at 25 °C. For dynamic quenching, the maximum collisional quenching constant obtained for various quenchers is 2.0 x 10^{10} M^{-1} s^{-1} (Aslanoglu *et al.*, 2005). However, k_q is much larger, suggesting that the quenching is due to the formation of a complex between KTZ and BSA, i.e., static quenching (Wang *et al.*, 2009).

The apparent binding constant (K_A) and the binding stoichiometry (n) (Table 1) of BSA–KTZ complex can be estimated by using the following relationship (Sun *et al.*, 2012):

$$\log (F_0 - F) / F = \log K_A + n \log [Q]$$

The value of K_A = 6.32 x 10^3 (t = 25°C) and the stoichiometry n = 0.98 was obtained from the intercept and slope of the plot of $\log [(F_0 - F)/F]$ versus $\log [Q]$ (Fig. 5c) respectively. Because K_A is lower than that of classical intercalative binding mode, groove binding is more reasonable.

Thermodynamic parameters and binding forces

The main binding forces between a small molecule and macromolecules in aqueous solution include van der Waals and electrostatic interactions as well as the hydrophobic effect, i.e., the release of water molecules from the solvation shell to the bulk solvent. Timasheff *et al.* (1972) and Ross *et al.* (1981) characterized the relationship between the sign and magnitude of the changes in thermodynamic parameters (ΔH and ΔS) and the kind of binding forces involved.In order to calculate ΔH and ΔS, van't Hoff equation, $ln\ K_{A2}/K_{A1} = (1/T_1 - 1/T_2)\ \Delta H/R$ was used. The Gibbs free energy change (ΔG) was determined from the binding constant at a particular temperature according to equation, $\Delta G = -RT\ ln\ K_A$, and ΔS were estimated according to equation $\Delta G = \Delta H - T\Delta S$. K_{A1} and K_{A2} are the binding constants at temperatures T_1 (298 K) and T_2 (308 K), respectively. The calculated negative value of ΔG revealed that the interaction between KTZ and BSA is spontaneous in aqueous solution. Negative value of ΔH was of hydrophobic interaction and positive value of ΔS (Table 1) indicates that the binding process is mainly entropy driven. The fact that ΔH and ΔS are both positive suggests a strong contribution of the hydrophobic effect (Bi *et al.*, 2009).

Absorption studies

The binding of KTZ to BSA was also characterized using the absorption titration. Figure 6a shows the electronic absorption spectrum of KTZ and the effect of BSA addition on the spectrum. One band centered at 246 nm dominated UV region of the electronic spectrum of KTZ. The absorbance of KTZ increased slightly with successive additions of BSA, suggesting that there exists an interaction between KTZ and BSA which is different from the intercalation binding mode. Classical intercalation has been characterized by large changes in the absorbance intensity and wavelength, whereas groove binders always display small changes (Kalanur *et al.*, 2009).

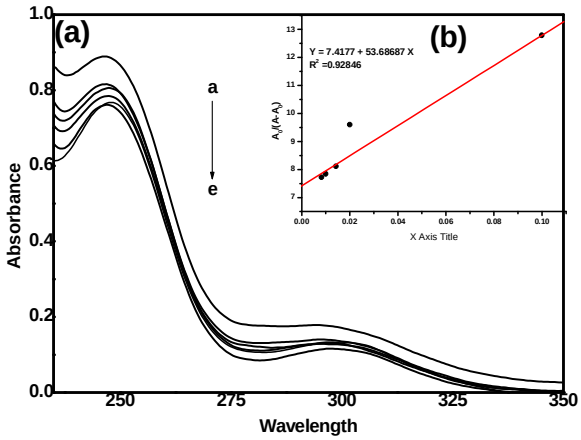

Fig. 6 (a) UV-visible spectra of 1x10^{-4} M KTZ in presence of C_{BSA} = 0, 10, 50, 70, 100, 120 μML^{-1} BSA in phosphate buffer solution pH 7.4 and **(b)** Plot of $(A_0/(A-A_0)$ versus 1/[Q].

As a consequence, groove binding is suggested as the main mode of interaction of KTZ with BSA. The binding constant, K was determined from the spectroscopic titration data using the following equation, $[BSA]/(\varepsilon_A-\varepsilon_f) = [BSA]/(\varepsilon_B-\varepsilon_f) + 1/K(\varepsilon_B-\varepsilon_f)$ where, ε_A, ε_f and ε_B correspond to $A_{obs}/[KTZ]$, the extinction coefficient for the free KTZ and the extinction coefficient for the KTZ in the fully bound form respectively. In the plot, (Fig. 6b), K_b is given by the ratio of the slope to the intercept. The binding constant, K_b, obtained for the KTZ–BSA interaction is 1.086 x 10^4 LM^{-1} at 25°C. The value of the binding constant, determined

using spectroscopic titration, is very close to the binding constant obtained by a static approach measuring fluorescence.

Molecular docking

Molecular docking technique is an attractive scaffold to understand the ligand-protein interactions which can substantiate our experimental results. Descriptions of the 3-D structure of crystalline albumin have revealed that BSA is made up of three homologous domains (I, II and III) was performed to study the interaction between KTZ and BSA and to determine the preferred binding site and binding mode. The best confirmation was determined based on binding affinity and RMSD. The binding energy and RMSD was performed by Auto Dock Vina.

The Docked conformation of the most active pose of KTZ in binding site shows total docking score of 4.0428. Molecular docking of KTZ on BSA was shown in 3-D docked structure (Fig. 7). The structure was studied for various inter molecular interaction and to determine the binding energy analysis of the docked complex. The KTZ was docked with receptor BSA using the parameters mentioned above. The energy obtained for KTZ-BSA complex was -10.0 Kcal/mol.

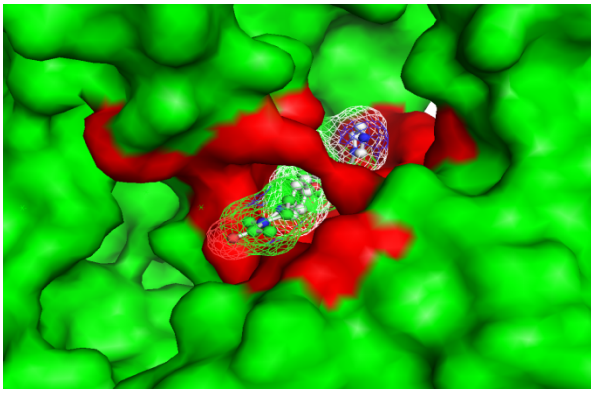

Fig. 7: Molecular model of the surface and the active site of the complex of KTZ (stick) and BSA (Green surface)

Viscosity measurements

In addition to voltammetric, fluorescence and UV absorption titration, viscosity measurements were carried out to provide further clues about a binding mode between KTZ and BSA. Classical intercalation results in lengthening of BSA due to the separation of base-pairs at the intercalation site, which produces a concomitant increase in the relative specific viscosity of such solutions.

Thus, such studies offer the least ambiguous test of intercalation (Lerman L. S., 1961, Satyanarayana *et al.*, 1992 and Kelly *et al.*, 1985). Minor positive or negative changes in BSA solution viscosity are observed when binding occurs in the BSA grooves (Kelly *et al.*, 1985). Fig. 8 shows the plot of flow time (*t*) of BSA with increasing concentrations of KTZ. It is observed that the addition of KTZ to BSA solution results in a slight increase in the flow time which is not as pronounced as observed for a classical intercalator (Vaidyanathan *et al.*, 2003) and is consistent with substrates that bind to BSA through a groove-binding mode via hydrophobic interaction (Metcalfe *et al.*, 2006).

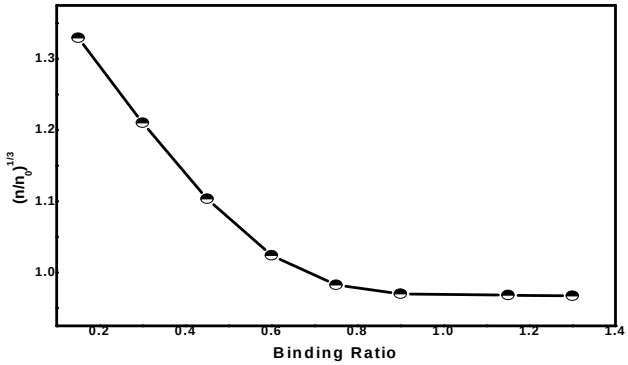

Fig. 8: Effect of BSA on the viscosity of KTZ solution at 100 µM L^{-1}, C_{BSA} = 0, 10, 20, 30, 40 and 50 µM L^{-1} phosphate buffer (0.1 M L^{-1}, pH 7.4) at 298 K.

CONCLUSION

The present work provides an approach for studying the interactions of BSA with ketokonazole using Voltammetry, absorption, fluorescence, viscometric and molecular modeling techniques under physiological conditions. The experimental results indicate that the probable quenching mechanisms of fluorescence of BSA by KTZ are static quenching procedure. The binding reaction of KTZ with BSA is mainly enthalpy driven, the electrostatic interactions play a major role in the reaction, in addition to the hydrophobic association. Since, the pharmaceutical firms need standardized screens for protein binding in the first step of new drug design, this kind of study of interaction between BSA with KTZ would be useful in pharmaceutical industry, life sciences and clinical medicine.

ACKNOWLEDGEMENTS

This work was financially supported by University Grants Commission (UGC), New Delhi, India (F. No. 42-308/2013 (SR) Dated 28/03/2013). Authors are very grateful thanks to Cipla Ltd., India for supplying gift sample of Ketoconazole. Thanks are also due to Dr. Siddalingeshwar, Department of Physics, MSRIT, Bangalore for providing spectrofluorimetric instrumental facility.

REFERENCES

Williams D, Feely J. Pharmacokinetic-pharmacodynamic drug interactions with HMG-CoA reductase inhibitors. J Clin Pharm, 2002; 41:343-370.

Carter DC, Ho JX. Structure of serum albumin. Adv Protein Chem, 1994;45:153-203.

He XM, Carter DC. Atomic structure and chemistry of human serum albumin. Nature, 1992;358: 209-215.

Zolese G, Falcioni G, Bertoli E, Galeazzi R, Wypych Z, Gratton E, Ambrosini A. Steady-state and time resolved fluorescence of albumins interacting with N-oleylethanolamine, a component of the endogenous N-acylethanolamines. Proteins, 2000;40:39-48.

Chadborn N, Bryant J, Bain A, O'Shea P. Ligand-dependent conformational equilibria of serum albumin revealed by tryptophan fluorescence quenching. Biophys J, 1999; 76:2198-207.

lson RE, Christ DD. Plasma protein binding of drugs. Ann Rep Med Chem, 1996; 31:327-336.

Hu YJ, Liu Y, Shen XS, Fang XY, Qu SS. Studies on the interaction between 1-hexylcarbamoyl-5-fluorouracil and bovine serum albumin. J Mol Struct, 2005;738:143-147.

Hu YJ, Liu Y, Wang JB, Xiao XH, Qu SS. Study of the interaction between monoammonium glycyrrhizinate and bovine serum albumin. J Pharm Biomed Anal, 2004;36:915-919.

Guharay J, Sengupta B, Sengupta PK. Protein-flavonol interaction: fluorescence spectroscopic study. Proteins, 2001;43:75-81.

Sulkowska A. Interaction of drugs with bovine and human serum albumin. J Mol Struct, 2002;614:227-232.

Gelamo EL, Tabak M**.** Spectroscopic studies on the interaction of bovine (BSA) and human (HSA) serum albumins with ionic surfactants**.** Spectrosc Acta Part A: Mol Biomol Spectrosc, 2000;56:2255-71.

Brockhinke A, Plessow R, Kohse-Höinghaus K and Herrmann C. Structural changes in the Ras protein revealed by fluorescence spectroscopy. Physical Chemistry Chemical Physics, 2003;5:3498-3506.

Lakowicz JR, 1999. Principles of Fluorescence Spectroscopy. New York, Kluwer Academic Publishers/Plenum Press, *2nd ed.*, 237-265.

Klajnert B, Bryszewska M. Fluorescence studies on PAMAM dendrimers interactions with bovine serum albumin. Bioelectrochemistry, 2002;55:33-35.

Sulkowska A, Rownicka J, Bojko B, Sulkowski W. Interaction of anticancer drugs with human and bovine serum albumin. J Mol Struct, 2003;651:653, 133-140.

Morris GM, Goodsell DS, Halliday RS. Automated Docking Using a Lamarckian Genetic Algorithm and and Empirical Binding Free Energy Function. J Comp Chem, 1998;19:1639-62.

Noel M, O'Boyle, Michael Banck. Open Babel: An open chemical toolbox, J of Cheminformatics, 2011;3:33.

Alasdair TR, Laurie, Richard M, Jackson. Q-SiteFinder: an energy-based method for the prediction of protein–ligand binding sites. Bioinformatics, 2005;21(9):1908-16.

Trott O, Olson AJ. AutoDock Vina: Improving the speed and accuracy of docking with a new scoring function, efficient optimization, and multithreading. J Compu Chem, 2010;31:455-461.

Bard AJ, Faulkner LR. 1980. Electrochemical methods: fundamentals and applications. New York 2nd ed,. Wiley**.**

Stela P, Florina P, Alexandru R, Biris, Stefania A, Valentin C, Gabriela B, Enkeleda D, Alexandru S Biris. Novel Graphene-Gold Nanoparticle Modified Electrodes for the high sensitivity Electrochemical Spectroscopy Detection and Analysis of Carbamazepine. J Phys Chem C, 2011;115:23387–23394.

Kalanur SS, Seetharamappa J. Elechtrochemical oxidation of bioxidative carbamazepine and its interaction with DNA. Anal Lett, 2010;43:618-630.

Laviron E. Adsorption auto inhibition and autocatalysis in polarography and linear potential sweep Voltammetry. J Electroanal Chem, 1974;52:355–393.

Laviron E. Adsorption autoinhibition and autocatalysis in polarography and linear potential. J Electroanal Chem, 1979;101:19–28.

Aslanoglu M. Electrochemical and spectroscopic studies of the interaction of proflavine with DNA. Anal Sci, 2006;22:439-43.

Li N, Ma Y, Yang C, Guo L, Yan X**.** Interaction of anticancer drug mitoxantrone with DNA analyzed by electrochemical and spectroscopic methods**.** Biophys Chem, 2005;116:199-205.

Shah A, Qureshi R, Janjua NK, Haque S, Ahmad S. Electrochemical and spectroscopic investigations of protonated ferrocene-DNA intercalation. Anal Sci, 2008;24:1437-41.

Aslanoglu M, Ayne G. Voltammetric studies of the interaction of Quinacrine with DNA. Anal Bioanal Chem, 2004;380:658-663.

Aslanoglu M, Oge N. Voltammetric, UV absorption and viscometric studies of the interaction of norepinephrine with DNA. Turk J Chem, 2005;29:477.

Wang, YQ, Zhang HM, Zhou QH, Xu HL. A study of the binding of colloidal Fe_3O_4 with bovine hemoglobin using optical spectroscopy. Colloid. Surface A, 2009; 337:102–108.

Sun Y, Ji F, Liu R, Lin J, Xu Q, Gao C. Interaction mechanism of 2- aminobenzothiazole with herring sperm DNA. J Lumin, 2012;132:507-512.

Shi Y, Guo C, Sun Y, Liu Z, Xu F, Zhang Y, Wen, ZLi. Interaction between DNA and micro cysteine-LR studied by spectra analysis and atomic force microscopy. Biomacromolecules, 2011;12:797-803.

Timasheff SN, Peeters H. 1972. Proteins of Biological Fluids. Pergamon Press, Oxford, 511-519.

Ross PD, Subramanian S. Thermodynamics of protein association reactions: forces contributing to stability. Biochemistry, 1981, 20, 3096-3102.

Bi SY, Sun YT, Qiao CY, Zhang HQ, Liu CM. Binding of several antitumor drugs to bovine serum albumin: Fluorescence study. J Lumin, 2009;129:541-547.

Kalanur SS, Katrahalli U, Seetharamappa J. Electrochemical studies and spectroscopic investigations on the interaction of an anticancer drug with DNA and their analytical applications. J Electroanal Chem, 2009;636:93-100.

Lerman LS. Structural considerations in the interaction of DNA and acridines. J Mol Biol, 1961;3:18-30.

Satyanarayana S, Dabrowiak JC, Chaires JB. Neither delta- nor lambda-tris(phenanthroline)ruthenium(II) binds to DNA by classical intercalation. Biochemistry, 1992;31:9319-24.

Kelly JM, Tossi AB, McConnell DJ, OhUigin C. A study of the interactions of some polypyridylruthenium (II) complexes with DNA using fluorescence spectroscopy, topoisomerisation and thermal denaturation. Nucleic Acids Res, 1985;13:6017-34.

Vaidyanathan VG, Nair BU. Photooxidation of DNA by a cobalt(II) tridentate complex. J Inorg Biochem, 2003;94:121-126.

Metcalfe C, Rajput C, Thomas JA. Studies on the interaction of extended terpyridyl and triazine metal complexes with DNA. J Inorg Biochem, 2006;100:1314-1319.

How to cite this article:

Babu Gowda, Mallappa M., Jayant I. Gowda, Raghavendran Rengasamy. Interaction of Ketoconazole with Bovine Serum Albumin: Electrochemical, Spectroscopic and Molecular Modeling Studies. J App Pharm Sci, 2015; 5 (Suppl 2): 037-044.